Inorg. Chem. **2005**, *44*, 4372–4382

Proton NMR Spectroscopy and Magnetic Properties of a Solution-Stable Dicopper(II) Complex Bearing a Single μ-Hydroxo Bridge

Iryna A. Koval,[†] Karlijn van der Schilden,[†] Anna Maria Schuitema,[†] Patrick Gamez,[†] Catherine Belle,[‡] Jean-Louis Pierre,[‡] Matthias LUken,[§] Bernt Krebs,[§] Olivier Roubeau,[||] and Jan Reedijk*,[†]

Leiden Institute of Chemistry, Leiden University, P.O. Box 9502, 2300 RA Leiden, The Netherlands, LEDSS, Chimie Biomimétique, UMR CNRS 5616, ICMG FR CNRS 2607, Université J. Fourier, B. P. 53, 38041 Grenoble Cedex, France, Institut für Anorganische und Analytische Chemie der Westfälischen Wilhelms-Universität Münster, Wilhelm-Klemm-Strasse 8, D-48149 Münster, Germany, and Centre de Recherche Paul Pascal-CNRS UPR 8641, 115 avenue du Dr. A. Schweitzer, 33600 Pessac, France

Received February 2, 2005

The reaction of copper(II) perchlorate with the macrocyclic ligand [22]py4pz in the presence of base leads to formation of a dinuclear complex $[Cu_2([22]py4pz)(\mu\text{-}OH)](ClO_4)_3 \cdot H_2O$, in which two copper ions are bridged by a single μ-hydroxo bridge. Each copper ion is further surrounded by four nitrogen atoms of the ligand. The μ-hydroxo bridge mediates a strong antiferromagnetic coupling ($2J = -691(35)$ cm^{-1}) between the metal centers, leading to relatively sharp and well-resolved resonances in the ^{1}H NMR spectrum of the complex in solution. We herein report the crystal structure, the magnetic properties, and the full assignment of the hyperfine-shifted resonances in the NMR spectrum of the complex, as well as the determination of the exchange coupling constant in solution through temperature-dependent NMR studies.

Introduction

Dinuclear copper(II) complexes with nitrogen-containing ligands have received great attention from the scientific community during the past decades.[1−6] The interest in these types of compounds is to a large extent caused by their resemblance to the active sites of several copper-containing proteins, especially those holding the type-3 active site. Besides that, the investigation of the magnetic properties of such complexes provides more insight into the relationship between their structural features and the strength of magnetic exchange interactions between the metal ions.

As a part of our interest in model compounds for the type-3 active site of copper proteins, we prepared and structurally characterized a new dinuclear copper(II) complex $[Cu_2([22]py4pz)(\mu\text{-}OH)](ClO_4)_3 \cdot H_2O$ (**1**) with the macrocyclic ligand [22]py4pz (Figure 1).[7] In this complex, two copper ions are kept together by the macrocyclic moiety, each copper ion being surrounded by four nitrogen donor atoms from the ligand. In addition, the copper(II) ions are bridged by a single hydroxo bridge. The structure of the complex is thus fairly similar to the met-form of the active site of catechol oxidase, a copper enzyme with the type-3 active site.[8] Realizing the strong power of proton NMR spectroscopy as a tool to study paramagnetic copper(II) complexes in solution, we now report the magnetic properties, as well as proton NMR studies, of the paramagnetic complex **1**.

Experimental Section

All starting materials were commercially available and used as purchased, unless stated otherwise. THF and methanol were dried

* Author to whom correspondence should be addressed. E-mail: reedijk@chem.leidenuniv.nl. Fax: +31 71 527 42 61.
[†] Leiden University.
[‡] Université J. Fourier.
[§] Universität Münster.
[||] CNRS UPR 8641.

(1) Torelli, S.; Belle, C.; Gautier-Luneau, I.; Pierre, J. L.; Saint-Aman, E.; Latour, J. M.; Le Pape, L.; Luneau, D. *Inorg. Chem.* **2000**, *39*, 3526−3536.
(2) Torelli, S.; Belle, C.; Hamman, S.; Pierre, J. L.; Saint-Aman, E. *Inorg. Chem.* **2002**, *41*, 3983−3989.
(3) Selmeczi, K.; Reglier, M.; Giorgi, M.; Speier, G. *Coord. Chem. Rev.* **2003**, *245*, 191−201.
(4) Thirumavalavan, M.; Akilan, P.; Kandaswamy, M.; Kandaswamy Chinnakali; Senthil Kumar, G.; Fun, H. K. *Inorg. Chem.* **2003**, *42*, 3308−3317.
(5) Börzel, H.; Comba, P.; Pritzkow, H. *Chem. Commun.* **2001**, 97−98.
(6) Monzani, E.; Battaini, G.; Perotti, A.; Casella, L.; Gullotti, M.; Santagostini, L.; Nardin, G.; Randaccio, L.; Geremia, S.; Zanello, P.; Opromolla, G. *Inorg. Chem.* **1999**, *38*, 5359−5369.
(7) Schuitema, A. M.; Aubel, P. G.; Koval, I. A.; Engelen, M.; Driessen, W. L.; Reedijk, J.; Lutz, M.; Spek, A. L. *Inorg. Chim. Acta* **2003**, *355*, 374−385.
(8) Klabunde, T.; Eicken, C.; Sacchettini, J. C.; Krebs, B. *Nat. Struct. Biol.* **1998**, *5*, 1084−1090.

10.1021/ic0501770 CCC: $30.25
Published on Web 05/07/2005

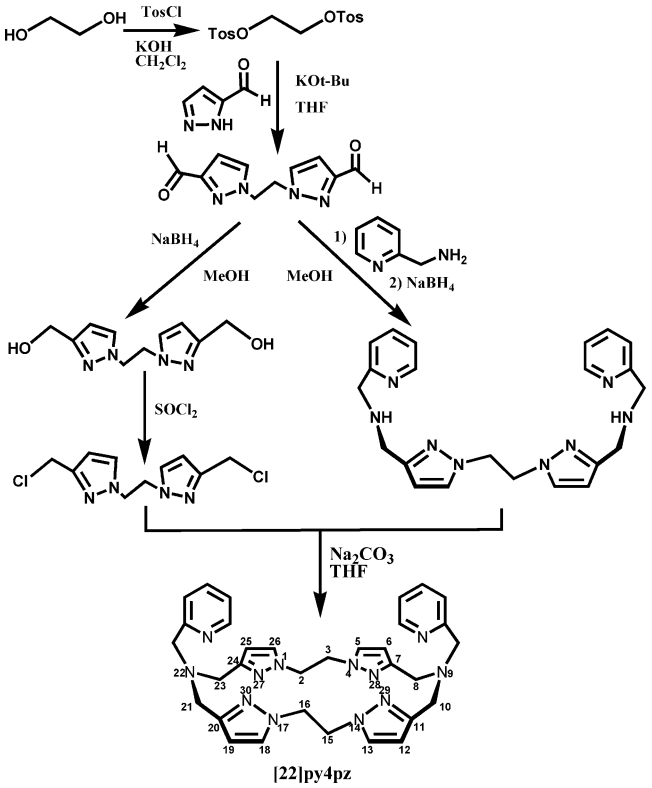

Figure 1. Scheme for the synthesis of the macrocyclic ligand [22]py4pz (9,22-bis(pyridin-2′-ylmethyl)-1,4,9,14,17,22,27,28,29,30-decaazapentacyclo[22.2.1.1^{4,7}.1^{11,14}.1^{17,20}]triacontane5,7(28),11(29),12,18,20(30),2(27),25-octaene).

over Na and distilled under Ar prior to use. The macrocyclic ligand [22]py4pz was synthesized as previously described.[7] The deuterated ligand [22]py4pz-d_8 was synthesized by following a similar experimental procedure, starting from the commercially available ethylene glycol-d_4. The infrared spectrum of **1** in the 4000−300 cm^{-1} range was recorded on a Bruker 330V IR spectrophotometer equipped with a Golden Gate Diamond. The ligand field spectrum in solution was recorded on a Varian Cary 50 Scan UV−vis spectrophotometer. Electrospray mass spectra (ESI-MS) in D_2O solutions were recorded on a Thermo Finnigan AQA apparatus. X-band electron paramagnetic resonance (EPR) measurements were performed at 77 K in the solid state on a JEOL RE2x electron spin resonance spectrometer, using DPPH ($g = 2.0036$) as a standard. Bulk magnetization measurements were performed on polycrystalline sample of **1** in the temperature range 5−400 K with a Quantum Design MPMS-5S SQUID magnetometer, in a 1 kG applied field. The data were corrected for the experimentally determined contribution of the sample holder. Corrections for the diamagnetic response of the complex, as estimated from Pascal's constants, were applied.[9]

^{1}H NMR Spectroscopic Studies. The ^{1}H 1D and 2D COSY NMR spectra were recorded on a DPX300 Bruker spectrometer. All chemical shifts were reported with respect to the residual solvent peak. The longitudinal relaxation times (T_1) were determined by standard inversion−recovery experiments, with 2 s relaxation delay and the spectral width of 99.7582 ppm. The COSY spectrum was obtained at 263 K by collecting 1024 F_2 × 1024 F_1 data points, with a mixing time of 20 ms, the relaxation delay of 0.02 s, and the spectral width of 34.0678 ppm. A total of 384 scans were collected. The NOE difference spectra were recorded on a DMX600 Bruker spectrometer. 1D NOE difference experiments were performed by a literature procedure,[10,11] using a frequency list to define irradiation frequencies, alternating on and off resonance every other scan. A WEFT pulse sequence was not applied. The irradiation time was 500 ms. The number of scans during the experiments was 4 k.

X-ray Crystal Structure Determination. X-ray diffraction intensities of **1** were measured on a Bruker AXS Apex diffractometer with a graphite monochromator. The structure was solved with direct methods (SHELXS97).[12] The structure refinement was done with SHELXL97[13] against F^2 of all reflections. Molecular illustrations, checking for higher symmetry and geometry calculations, were performed with the PLATON[14] package.

Safety Note. *Although no problems were encountered during the preparation of perchlorate salts, these compounds are potentially hazardous and should be treated with care.*

Synthesis of 1,2-Bis(tosyloxy)ethane-d_4. The compound was synthesized in the same way as its nondeuterated analogue, starting from commercially available ethylene glycol-d_4.[15] Yield: 82.8%. ^{1}H NMR (300 MHz, DMSO, ppm): 7.71 (d, 4H, Ar-(*o*)-*H*); 7.45 (d, 4H, Ar-(*m*)-*H*); 2.44 (s, 6H, Ar-C*H*$_3$).

Synthesis of 1,2-Bis(3′-formylpyrazol-1′-yl)ethane-d_4. The compound was synthesized as a white solid by the same method as its nondeuterated analogue.[15] Yield: 58%. ^{1}H NMR (300 MHz, $CDCl_3$, ppm): 9.97 (s, 2H, C(O)*H*); 7.08 (d, 2H, 4′-pz-*H*); 6.69 (d, 2H, 5′pz-*H*).

Synthesis of 1,2-Bis(3′-(hydroxymethyl)pyrazol-1′-yl)ethane-d_4. The compound was synthesized by the same method as its nondeuterated analogue and used without purification from borate salts.[15] Yield: not determined (above 100% due to the presence of borate salts). ^{1}H NMR (300 MHz, $CDCl_3$, ppm): 7.13 (d, 2H, 4′-pz-*H*); 6.16 (d, 2H, 5′-pz-*H*); 4.54 (s, 4H, pz-C*H*$_2$-OH).

Synthesis of 1,2-Bis(3′-(chloromethyl)pyrazol-1′-yl)ethane-d_4. The compound was synthesized by a modified procedure. The white solid obtained in the synthesis of 1,2-bis(3′-(hydroxymethyl)pyrazol-1′-yl)ethane-d_4 was dissolved in 100 mL of thionyl chloride and heated at 50 °C upon stirring for 24 h. Afterward, $SOCl_2$ was evaporated under reduced pressure, and the residue was neutralized with saturated aqueous solution of Na_2CO_3. The product was extracted with dichloromethane. The organic phase was dried upon Na_2SO_4 and evaporated under reduced pressure. The product was recrystallized from methanol. Yield: 45% (relative to 1,2-bis(3′-formylpyrazol-1′-yl)ethane-d_4). ^{1}H NMR (300 MHz, $CDCl_3$, ppm): 6.90 (d, 2H, 4′-pz-*H*); 6.16 (d, 2H, 5′-pz-*H*); 4.59 (s, 4H, pz-C*H*$_2$-Cl).

Synthesis of 1,2-Bis(3′-((2-pyridine-2-ylmethyl)amino)-1′-pyrazolyl)ethane-d_4 (py2pz-d_4). The compound was synthesized according to the procedure used for its nondeuterated analogue.[15] Yield: 64%. ^{1}H NMR (300 MHz, $CDCl_3$, ppm): 8.53 (d, 2H, 6′-*H*-py), 7.63 (td, 2H, 4′-*H*-py); 7.34 (d, 2H, 3′-*H*-py); 7.13 (td, 2H, 5′-*H*-py), 6.90 (d, 2H, 5′-*H*-pz); 6.08 (d, 2H, 4′-*H*-pz); 3.95 (s, 4H, py-C*H*$_2$-N); 3.85 (s, 2H, pz-C*H*$_2$-N).

Synthesis of 9,22-Bis(pyridin-2-ylmethyl)-1,4,9,14,17,22,27,28,29,30-decaazapentacyclo[22.2.1.1^{4,7}.1^{11,14}.1^{17,20}]triacontane-5,7(28),11(29),12,18,20(30),24(27),25-octaene ([22]py4pz-d_8). The compound was synthesized by a modified procedure. A 0.301 g (2.84 mmol) amount of sodium carbonate and 0.577 g (1.42 mmol)

(9) Kolthoff, I. M.; Elving, P. J. *Treatise on Analytical Chemistry*; Interscience Encyclopedia, Inc.: New York, 1963.

(10) Dugad, L. B.; La Mar, G. N. *Biochemistry* **1990**, *29*, 2263−2271.

(11) Banci, L.; Bertini, I.; Luchinat, C.; Piccioli, M.; Scozzafava, A.; Turano, P. *Inorg. Chem.* **1989**, *28*, 4650−4656.

(12) Sheldrick, G. M. *SHELXS-97, Program for crystal structure solution*; University of Göttingen: Göttingen, Germany, 1997.

of py2pz-d_4 were suspended in 3000 mL of dry THF. The reaction mixture was cooled to −40 °C, and a solution of 0.374 g (1.42 mmol) of 1,2-bis(3′-(chloromethyl)pyrazol-1′-yl)ethane-d_4 in ca. 200 mL of THF was added. The reaction mixture was allowed to warm slowly to RT (room temperature) and was then refluxed for 14 days under Ar. After 2 weeks, the solvent was evaporated, and the residue was redissolved in ca. 500 mL of a CH_2Cl_2−water mixture (1:1 v:v). The aqueous phase was acidified with 35% HCl (pH = 1) and washed a few times with dichloromethane. Afterward, the aqueous layer was basified with NH_4OH (pH = 9), and the product was extracted a few times with dichloromethane. The combined organic layers were dried over Na_2SO_4, and the solvent was evaporated. The obtained yellow oil was redissolved in methanol, and the product was precipitated with diethyl ether. Yield: 27%. ^{1}H NMR (300 MHz, $CDCl_3$, ppm): 8.40 (d, 2H, 6′-*H*-py), 7.81 (td, 2H, 4′-*H*-py); 7.64 (d, 2H, 3′-*H*-py); 7.41 (d, 2H, 5′-*H*-pz); 7.25 (td, 2H, 5′-*H*-py); 6.11 (d, 2H, 4′-*H*-pz); 3.56 (s, 4H, py-CH_2-N); 3.36 (s, 2H, pz-CH_2-N).

Synthesis of (3-Methylpyridin-2-yl)methylamine Dihydrochloride. The compound was synthesized according to a slightly modification of the procedure reported earlier by Fos et al.[16] A 1 g amount of 2-cyano-3-methylamine was dissolved in 200 mL of dry MeOH and hydrogenated with molecular hydrogen in the presence of 1.5 g of 10% Pd on charcoal. After 6 h, the charcoal was filtered off, and 4 mL of concentrated HCl was added to the resulting solution. After evaporation, a mixture of white crystals of product and some amount of light yellow oil was obtained. The product was recrystallized from a MeOH−diethyl ether mixture. Yield: 0.70 g (42%). ^{1}H NMR (MeOD, 300 MHz, ppm): 8.64 (d, 1H, 2′-*H*-py); 8.14 (d, 1H, 4′-*H*-py), 7.69 (dd, 1H, 3′-*H*-py), 4.45 (s, 2H, CH_2py), 2.52 (s, 3H, CH_3).

Synthesis of 1,2-Bis(3′-((3-methyl-2-pyridine-2-ylmethyl)-amino)-1′-pyrazolyl)ethane (py2Me$_2$pz). Under an argon atmosphere, 0.38 g (1.78 mmol) of 1,2-bis(3′-formylpyrazol-1′-yl)ethane and 1.2 mL (4 equiv) of diisopropylethylamine (DIPEA) were dissolved in 400 mL of dry methanol. A solution of 0.68 g (3.46 mmol) of (3-methylpyridin-2-yl)methylamine dihydrochloride in 50 mL of dry MeOH was added dropwise to the reaction mixture. The purity of the imine, which immediately forms in situ, was checked by NMR spectroscopy, and its reduction was carried out without isolating the compound. $NaBH_4$ (3 equiv/CH═N bond) was added to the solution. After the evolution of the gas stopped, the resulting mixture was refluxed for 2 h and the solvent was evaporated under reduced pressure. The residue was dissolved in ca. 250 mL of a shaking H_2O−dichloromethane mixture, and the organic layer was separated. After the aqueous layer was washed a few more times with dichloromethane, the organic layers were combined, dried over Na_2SO_4, and evaporated. This workup resulted in the pure product as a light yellow oil. Yield: 0.47 g (61%).

^{1}H NMR ($CDCl_3$, 300 MHz, ppm): 8.39 (d, 2H, 6′-*H*-py), 7.41 (d, 2H, 4′-*H*-py), 7.06 (dd, 2H, 5′-*H*-py), 6.90 (d, 2H, 3′-*H*-pz), 6.08 (d, 2H, 4′-*H*-pz), 4.47 (s, 4H, pz-(CH_2)$_2$-pz), 3.90 (s, 8H, NH-CH_2-py + NH-CH_2-pz), 2.32 (s, 6H, CH_3-py).

Synthesis of 9,22-Bis(3-methylpyridin-2-ylmethyl)-1,4,9,14, 17,22,27,28,29,30-decaazapentacycle[22.2.1.1^{4,7}.1^{11,14}.1^{17,20}]-triacontane-5,7(28),11(29),12,18,20(30),24(27),25-octaene ([22]-py-Me$_2$4pz). Under an argon atmosphere, 0.343 g (3.24 mmol) of Na_2CO_3 and 0.696 g (1.62 mmol) of py2Me$_2$pz were suspended in 3500 mL of dry THF. Then ca. 200 mL of CH_3CN was added to ensure the dissolution of the organic compound. The suspension was cooled to −20 °C, and a solution of 0.419 g (1.62 mmol) of 1,2-bis(3′-(chloromethyl)-1′-pyrazolyl)ethane in 100 mL of dry THF was added to the reaction mixture. The resulting suspension was allowed to warm slowly to room temperature and refluxed for 2 weeks under argon. Afterward, the solvent was evaporated, and the residue was redissolved in a dichloromethane−water mixture. The organic layer was separated, and the aqueous layer was washed three more times with dichloromethane. The product was extracted by a diluted HCl solution, and the resulting aqueous solution was washed a few more times with dichloromethane. Addition of an ammonium hydroxide solution until pH = 11 resulted in the formation of a white suspension, which was extracted four times with dichoromethane. The resulting organic solution was dried over Na_2SO_4 and evaporated under reduced pressure. The resulting crude product, obtained as a dark-brown oil, was purified by column chromatography on silica, using a CH_2Cl_2−MeOH mixture (85:15, v:v) as an eluent. The pure ligand was crystallized from a MeOH−diethyl ether solution and isolated as a white powder. Yield: <10%. ^{1}H NMR (300 MHz, MeOD, ppm): 8.35 (d, 2H, 6′-*H*-py); 7.68 (d, 2H, 4′-*H*-py); 7.49 (d, 2H, 5′-*H* -pz); 7.29 (d, 2H, 5′-*H*-py); 6.19 (d, 4H, 4′-*H*-pz); 4.57 (s, 16H, pz-(CH_2)$_2$-pz + pz-(CH_2)-N); 3.69 (s, 4H, py-CH_2-N); 2.28 (s, 6H, CH_3-pz)

Synthesis of [Cu$_2$([22]py4pz)(μ-OH)](ClO$_4$)$_3$·H$_2$O (1). A solution of $Cu(ClO_4)_2$·$6H_2O$ (74 mg, 0.20 mmol) in ca. 2 mL acetonitrile was added to a suspension of [22]py4pz (58 mg, 0.10 mmol) in the same solvent (the free ligand does not dissolve unless coordinated to the metal ions). To the resulting greenish-blue solution was added 1 equiv of NMe_4OH (20% solution in methanol), which resulted in an immediate color change to clear green. Small amounts of copper hydroxide that may precipitate occasionally were removed by filtration. The resulting clear solution was concentrated to the half of the initial volume. Diethyl ether diffusion led to small green crystals, which were isolated and recrystallized from an acetonitrile−diethyl ether mixture. Single crystals were obtained by slow diffusion of diethyl ether into a diluted acetonitrile solution of **1**. Anal. Found (calcd) for [Cu$_2$([22]py4pz)(μ-OH)](ClO$_4$)$_3$·H$_2$O ($C_{32}H_{39}Cl_3Cu_2N_{12}O_{14}$): C, 36.6 (36.6); H, 3.7 (3.3); N, 16.0 (15.6). IR (4000−300 cm^{-1}; ν): 3514 (O−H stretching), 3126 (C−H arom stretching), 1610 (C═N arom pyridine), 1515 (C═N arom pyrazole), 1076 (ClO_4^-)

Preparation of [Cu$_2$([22]pyMe$_2$4pz)(μ-OH)](ClO$_4$)$_3$·H$_2$O (1-Me$_2$) (in Situ). A solution of $Cu(ClO_4)_2$·$6H_2O$ (7.2 mg, 0.019 mmol) in ca. 1 mL of acetonitrile was added to a suspension of [22]py2Me4pz (6.0 mg, 0.010 mmol) in the same solvent (the ligand does not dissolve without coordination to metal ions). To the resulting green solution was added 1 equiv of NMe_4OH (20% solution in methanol), which resulted in an immediate color change to greenish-yellow. The resulting solution was concentrated until reaching half of the initial volume. Diethyl ether diffusion led to the formation of a very light-green amorphous powder, which was redissolved in D_2O and used for the NMR spectroscopic studies. The in situ formation of the hydroxo-bridged complex was confirmed by ESI-MS measurements (D_2O, *m*/*z* 529 (1[22]pyMe$_2$-4pz + 2Cu + 1OH + 3ClO$_4$, *z* = 2; 1078 (1[22]pyMe$_2$4pz + 2Cu + 1OH + 3ClO$_4$ + D_2O, *z* = 1) and UV−vis spectroscopy (in D_2O, λ = 350 nm (CT Cu(II) ← OH).

Results and Discussion

Synthesis and Physical Properties of 1. The dinuclear complex [Cu$_2$([22]py4pz)OH](ClO$_4$)$_3$·H$_2$O was prepared by

(13) Sheldrick, G. M. *SHELXL-97, Program for the refinement of crystal structures*; University of Göttingen: Göttingen, Germany, 1997.
(14) Spek, A. L. *J. Appl. Crystallogr.* **2003**, *36*, 7−13.
(15) Schuitema, A. M. Ph.D. Thesis, Leiden University, 2004.
(16) Fos, E.; Bosca, F.; Mauleon, D.; Carganico, G. *J. Heterocycl. Chem.* **1993**, *30*, 473−476.

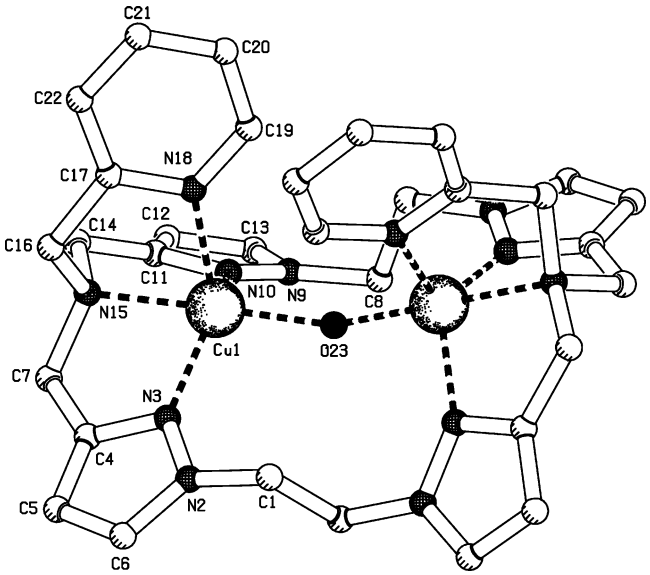

Figure 2. Platon[14] representation of the complex cation $[Cu_2([22]py4pz)(\mu\text{-}OH)]^{3+}$. Hydrogen atoms are omitted for clarity.

reaction of $Cu(ClO_4)_2 \cdot 6H_2O$ and the ligand [22]py4pz in acetonitrile in the presence of 1 equiv of NMe_4OH. Small green crystals of the compound, suitable for X-ray single crystal analysis, were obtained by slow diethyl ether diffusion in an acetonitrile solution of the complex. The complex was found to be moderately soluble in acetonitrile and DMSO, poorly soluble in water, and completely insoluble in other common solvents.

The UV−vis−NIR spectrum of the complex in CH_3CN solution exhibits two absorption bands at 350 nm ($\epsilon = 7176$ M^{-1} cm^{-1}) and at 821 nm ($\epsilon = 336$ M^{-1} cm^{-1}). The first one corresponds to the charge-transfer band from the hydroxo bridge to the copper ions, whereas the second one is assigned to a d−d transition band of Cu(II) ions. The complex is EPR silent in either the solid state or in acetonitrile solution at 77 K.

Crystal Structure Description of 1. The molecular structure[14] of **1** is depicted in Figure 2. Selected bond distances and bond angles are presented in Table 1. The asymmetric unit comprises half a cation $[Cu_2([22]py4pz)OH]^{3+}$; the other half of the cation is generated through a symmetry operation: (a) $1 - x, y, {}^1/_2 - z$.

The Cu(II) ion is in an N_4O environment which can be best described as distorted trigonal bipyramid with the τ value of 0.83 ($\tau = 1$ for the trigonal bipyramidal geometry and 0 for the square pyramidal geometry).[17] The equatorial positions are occupied by the two pyrazole nitrogen atoms, N3 and N10 at distances of respectively 2.033(3) and 2.072(3) Å, and the pyridine N18 atom at a distance of 2.087(4) Å. The bridging O23 atom at a distance of 1.9215(12) Å and the tertiary amine N15 atom at a distance of 2.065(3) Å are occupying the axial positions. The small N3−Cu1−N15 and N15−Cu1−N10 angles of 80.17(13) and 80.94(13)°, respectively, are imposed by the three-bond ligand bites. The bridging oxygen atom O23 from the hydroxide anion

Table 1. Selected Bond Lengths and Angles for $[Cu_2([22]py4pz)(\mu\text{-}OH)](ClO_4)_3 \cdot H_2O$ (1)[a]

Bond Distances (Å)			
Cu1···Cu1a	3.7587(11)	Cu1−N15	2.065(3)
Cu1−O23	1.9215(12)	Cu1−N10	2.072(3)
Cu1−N3	2.033(3)	Cu1−N18	2.087(4)
Bond Angles (deg)			
Cu1−O23−Cu1a	156.0(3)	N15−Cu1−N10	80.94(13)
O23−Cu1− N3	98.55(11)	O23−Cu1−N18	100.85(16)
O23−Cu1−N15	178.60(14)	N3−Cu1−N18	122.50(14)
N3−Cu1−N15	80.17(13)	N15−Cu1−N18	80.36(14)
O23−Cu1−N10	99.49(11)	N10−Cu1−N18	100.38(13)
N3−Cu1−N10	128.73(13)		

[a] Symmetry code: (a) $1 - x, y, -z + 1/2$.

connects the two central copper atoms Cu1 and Cu1a, whereby the macrocycle adopts a cis-(boat) conformation. The two pyridine groups are located at the same side above the macrocyclic ring, and the two Cu(II) ions lie almost in the plane of the ring with a Cu−Cu distance of 3.7587(11) Å. The Cu−O−Cu angle is 156.0(3)°.

Magnetic Behavior of 1. The temperature dependence of the molar magnetic susceptibility χ_M and its inverse $1/\chi_M$ deduced from measurements at 1000 Oe are given in Figure 3.[18] The molar magnetic susceptibility χ_M of compound **1** at 350 K equals ca. 5×10^{-4} cm^3 mol^{-1}, about half of the expected value for two uncoupled $S = 1/2$ centers (ca. 1×10^{-3} cm^3 mol^{-1}), thus indicating strong antiferromagnetic coupling between copper(II) ions. Upon lowering of the temperature, χ_M further decreases to reach a plateau at ca. 1.5×10^{-4} cm^3 mol^{-1} below 150 K. At temperatures below 100 K, the behavior is dominated by a Curie tail typical of a small paramagnetic impurity, often found in copper molecular compounds. The presence of a small paramagnetic impurity is confirmed by measurements against the applied field at 5 and 100 K (Figure S1, Supporting Information). To evaluate the strength of the magnetic interaction between the copper(II) ions within the dimeric unit in **1**, the following expression for the susceptibility, based on the Hamiltonian $H = -2JS_1S_2$ was thus used:[19]

$$\chi = (1-p)\frac{2N_A\beta^2g^2}{k_BT\left[1+3\exp\left(-\frac{2J}{k_BT}\right)\right]} + 2p\frac{N_A\beta^2g^2}{k_BT} + \mathrm{TIP}$$

Here $2J$ corresponds to the singlet−triplet energy gap, p represents the amount of paramagnetic impurity, and TIP is a temperature-independent paramagnetism term. Fitting was performed fixing g to 2, and the best-fit parameters were then $2J = -691(35)$ cm^{-1}, $TIP = 1.0(1) \times 10^{-4}$ cm^3 mol^{-1}, and $p = 0.63(1)\%$. The large error bar on $2J$ lies in the lack of data at higher temperatures at which the maximum in χ_M would be observed.

From the magneto−structural viewpoint, dinuclear copper complexes with a single hydroxo bridge are still rare, given the extensive research devoted to copper(II) coordination

(17) Addison, A. W.; Rao, T. N.; Reedijk, J.; van Rijn, J.; Verschoor, G. C. *J. Chem. Soc., Dalton Trans.* **1984**, 1349−1356.

(18) All data are given in cgs units. Since the magnetic susceptibility is dimensionless in the SI system, the conversion factor for molar magnetic susceptibility in SI units (mol^{-1}) is simply 4π.

(19) Kahn, O. *Molecular Magnetism*; Wiley-VCH: New York, 1993.

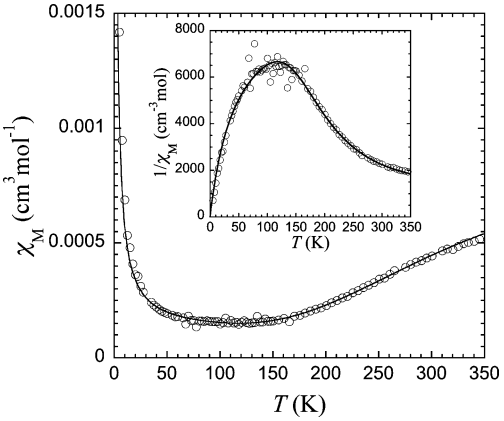

Figure 3. Magnetic susceptibility data χ and $1/\chi$ vs T for **1** in the temperature range 5−350 K in a 1000 Oe applied field. The full lines correspond to the best fit to a dimer model (see text).

compounds. In all cases, antiferromagnetic exchange couplings have been observed, the strength of which depends on structural parameters. Attempts to derive magneto−structural correlations were undertaken recently[20] for monohydroxo-bridged copper(II) ions in a square-planar environment. It was found that the antiferromagnetic exchange coupling increases with the Cu−O−Cu angle. Indeed for such geometry, the σ overlap of the spin-rich $d_{x^2-y^2}$ orbitals increases with Cu−O−Cu angles closer to 180°. In **1**, however, the Cu(II) ions are in a trigonal bipyramid environment with the hydroxo bridge in axial position. Furthermore, besides square-pyramidal and trigonal bipyramidal surroundings, monohydroxo-bridged copper(II) dimers are also found in the literature in combination with other bridging ligands and with tetrahedral, square pyramidal, octahedral environments, various types of distortions, and different coordination sites for the hydroxo bridge. Therefore, we have gathered in Table 2 and Figures 4 and S2 (Supporting Information) the reported magneto−structural data for dinuclear compounds in which the Cu(II) ions are only bridged by one hydroxo group and for which the geometry around the Cu(II) ions can be reasonably described by a type of coordination sphere. We have excluded cases for which spin density at the hydroxo coordination site is expected to be negligible, e.g. for the hydroxo-bridging group in axial position in a square-pyramidal geometry. There is a common general trend, with the singlet−triplet energy gap increasing with longer Cu···Cu separations, wider Cu−O−Cu angles, and higher Cu−O−Cu/Cu···Cu ratios. These structural parameters are obviously interdependent. For the three geometries considered, the increase in singlet−triplet energy gap in fact corresponds to a variation of the structural parameters toward situations for which overlap between the magnetic orbitals (d_{z^2} in trigonal bipyramid, $d_{x^2-y^2}$ in square planar and square pyramid) and the hydroxo O 2p orbital is the most efficient, close to linearity. The antiferromagnetic σ-superexchange pathway through the hydroxo bridge is then the most efficient, yielding virtually diamagnetic complexes. In addition, there is a good linear correlation between the Cu···Cu separation and the singlet−triplet energy gap among compounds having trigonal bipyramid geometry and the hydroxo bridge in axial position and square pyramidal geometry with the hydroxo bridge in the equatorial position (see Figure 3, left). It has to be noted that, for such a monatomic single bridge, only a small dependence on the actual Cu(II) coordination environment can be expected, if the bridging atom lies in a spin-rich position. The correlation found here is of relevance for the characterization of mimics of dinuclear copper centers from biology.

^{1}H NMR Assignment Strategy for 1. ^{1}H NMR, 2D COSY NMR and T_1 Measurements. ^{1}H NMR spectroscopy has only relatively recently emerged as a useful tool in studying the structural and magnetic properties of Cu(II) coordination compounds in solution.[21−23] The slow electronic relaxation of Cu(II) ions usually results in large line widths and poor resolution of the spectra, which makes their interpretation very difficult, if not impossible. However, if two antiferromagnetically coupled copper(II) ions are present in a complex, the situation is different. In antiferromagnetically coupled dicopper(II) systems, the ground state is a diamagnetic ($S = 0$) singlet. The energy separation between the ground state and the paramagnetic ($S = 1$) excited triplet state, which increases with the strength of the antiferromagnetic coupling, may lead to relatively sharp resonances, facilitating the spectra interpretation.[24]

In our case, a very strong ($2J = -691(35)$ cm^{-1}) antiferromagnetic coupling between the copper(II) centers in **1** results in relatively sharp resonances with rather small hyperfine shifts, observed in a range of −50 to +30 ppm.

At room temperature, only 7 well-resolved signals are found in the region of 0−200 ppm in the ^{1}H NMR spectrum of **1** (Figure 5). One additional weak signal is observed at −48 ppm (Figure 6, left). The temperature-variable 1D spectra, recorded in the temperature interval 233−353 K (Figure 6, the data recorded above 293 K are not shown), reveal that the signal observed at 8.6 ppm at RT results from coincidental degeneracy of two resonances. Furthermore, two very broad signals at ca. 25 and 20 ppm become clearly visible at 233 K. In total, 11 resonances are thus observed in the whole spectral window (Figure 6), which implies the presence of an additional (pseudo) symmetry plane in the cationic species next to the C_2 symmetry axis, observed in the crystal structure of **1**. One can imagine it connecting two tripodal nitrogen atoms, passing through both copper centers and with two pyridine rings lying virtually in the plane, resulting in the equivalency of all four pyrazole rings, all methylene groups of the ethylene moeities, and the methylene N(tripodal)-CH_2-pz groups. However, taking into account that the two protons (e.g. equatorial vs axial) of the methylene groups are diastereotopic and that these usually experience different hyperfine shifts, 12 resonances are expected for **1**

(20) Patra, A. K.; Ray, M.; Mukherjee, R. *Polyhedron* **2000**, *19*, 1423−1428.

(21) Holz, R. C.; Brink, J. M. *Inorg. Chem.* **1994**, *33*, 4609−4610.

(22) Murthy, N. N.; Karlin, K. D.; Bertini, I.; Luchinat, C. *J. Am. Chem. Soc.* **1997**, *119*, 2156−2162.

(23) Brink, J. M.; Rose, R. A.; Holz, R. C. *Inorg. Chem.* **1996**, *35*, 2878−2885.

(24) Banci, L.; Bertini, I.; Luchinat, C. *Struct. Bonding* **1990**, *72*, 113−135.

Table 2. Magneto−Structural Data for Relevant Dicopper(II) Complexes with a Single Hydroxo Bridge[a]

formula	Cu···Cu (Å)	Cu−O−Cu (deg)	Cu−O−Cu/Cu···Cu (deg)	$2J$ (cm^{-1})	geometry type	ref
$[Cu_2(bpy)_4(OH)](ClO_4)_3$	3.645	141.60	38.85	−322	TBPeq	Haddad, 1981[41]
$Na[Cu_2(L^1)_2(OH)]\cdot 2H_2O$	3.437	131.11	38.15	−334	SPl	Patra, 2000[20]
$K[Cu_2(L^1)_2(OH)]\cdot 2H_2O$	3.370	125.74	37.31	−298	SPl	Patra, 2000[20]
$[Cu_2(L^2)(OH)](ClO_4)_3\cdot 1.5H_2O$	3.740	150.60	40.27	−510	TBPax	Adams, 1996[42]
$[Cu_2([22]py4pz)OH](ClO_4)_3\cdot H_2O$	3.757	155.97	41.49	−691	TBPax	this work
$[Cu_2(L^3)(OH)(ClO_4)](ClO_4)_2\cdot CHCl_3$	3.642	143.7	39.46	−500	SPy	Coughlin, 1981[43]
$[Cu_2(L^4)(OH)](CF_3SO_3)_3$	3.90	174.0	44.61	−865	TBPax	Lu, 1994[44]
$[Cu_2(L^4)(OH)](CF_3SO_3)_3\cdot H_2O$	3.90	174.0	44.61	−880	TBPax	Harding, 1993[45]
$[Cu_2(L^5)(dpm)(OH)](ClO_4)_3\cdot 2H_2O$	3.663	137.9	37.65	−365	SPy	Spodine, 1991[46]
$[Cu_2(L^6)(OH)](ClO_4)_2\cdot H_2O$	3.57	141.7	39.69	−240	SPy	Drew, 1981[47]
$[Cu_2(dien)_2(ClO_4)_3(OH)]$	3.435	128.1	37.29	−374	SPl	Castro, 1990[48]
$[Cu_2(terpy)_2(H_2O)(ClO_4)_3(OH)]$	3.642	145.7	40.05	−303	SPy	Folgado, 1989[49]
$[Cu_2(L^7)(OH)](CF_3SO_3)(BPh_4)_2$	3.89	166.1	42.70	−430	TBPeq	Harding, 1995[50]
$[Cu_2(tpmc)(OH)](ClO_4)_3\cdot 2H_2O$	3.712	134.5	36.23	−86	TBPeq	Asato, 1989[51]

[a] $2J$ represents here the singlet−triplet energy gap. SPl = square planar, Spy = square pyramidal with OH^- in equatorial position, TBPax = trigonal bipyramid with OH^- in axial position, TPBeq = distorted trigonal bipyramid with OH^- in equatorial position. H_2L^1 = 2,6-bis[*N*-(phenyl)carbamoyl]pyridine, L^2 = tetraimine Schiff base of tris(2-aminoethyl)amine and 2,5-diformylfuran, L^3 = 1,4,7,13,16,19-hexaaza-10,22-dioxatetracosane, L^4 = octaamine from BH_4^- reduction of the Schiff base of tris(2-aminoethyl)amine and 2,5-diformylfuran, L^5 = 1,1,2,2-tetrakis(2-pyridyl)ethylene, dpm = bis(2-pyridyl)methane, L^6 = Schiff base of 2,6-diacetylpyridine and 3,6-dioxaoctane-1,8-diamine, dien = diethylenetriamine, terpy = 2,2′;6′,2″-terpyridine, L^7 = partially hydrolyzed Schiff base of 2,6-diacetylpyridine and tris(2-aminoethyl)amine, and tpmc = 1,4,8,11-tetrakis(2-pyridylmethyl)-1,4,8,11-tetraazacyclotetradecane.

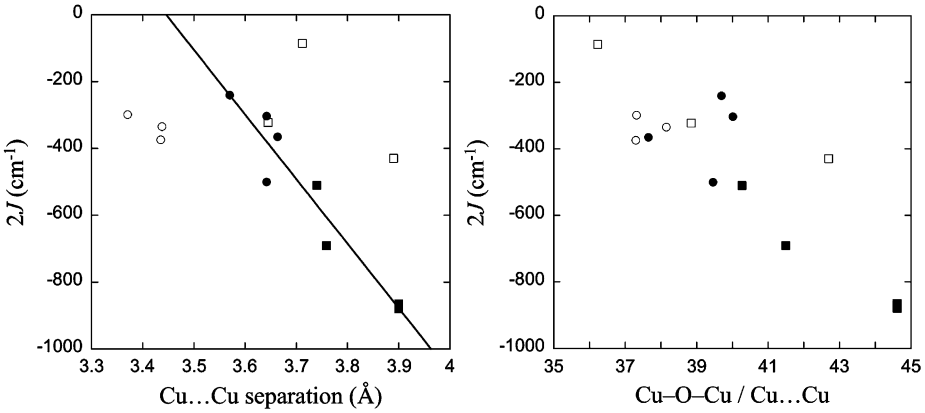

Figure 4. Correlation of the singlet−triplet energy gap $2J$ in monohydroxo-bridged dicopper(II) complexes with the Cu···Cu separation (left) and with the ratio Cu−O−Cu angle over Cu···Cu separation (right). Empty circles represent square planar geometry, full circles square pyramidal geometry with OH group in equatorial position, full squares trigonal bipyramid geometry with OH group in axial position, and empty squares trigonal bipyramid geometry with OH group in equatorial position. The full line is a linear fit (equation $-2J = 6653.8 - 1931.3 \times$ Cu···Cu) of the data concerning compounds with trigonal bipyramid geometry and the hydroxo bridge in an axial position and square pyramidal geometry with hydroxo bridge in an equatorial position.

(it should be noted that the protons of the pyridylmethylene moieties are *not* diastereotopic, as they become symmetry-related due to the pseudo symmetry plane). In general, the protons in a close proximity to copper ions experience stronger paramagnetic effect and thus shorter longitudinal relaxation times (T_1) and broader line widths (shorter transverse relaxation times T_2) in comparison to the protons in the periphery.[22] Therefore, as shown previously for paramagnetic Cu(II) complexes, it is not uncommon for the resonances corresponding to the protons closest to copper to broaden beyond recognition.[25,26] It can be thus tentatively proposed that the resonances corresponding to the methylene protons of the pyridylmethyl moieties, which are the closest to copper (H16a−Cu 3.050 Å, H16b−Cu 3.728 Å), are too broad to be detected. Another explanation of the observation of only 11 signals instead of 12 would be a coincidental degeneracy of two resonances which cannot be resolved at different temperatures due to the line broadness.

The peak at −48 ppm can easily be assigned to the proton of the OH group, as it has an approximate integral intensity of 1 and disappears upon addition of D_2O to the complex solution due to a proton−deuterium exchange. Furthermore, as evidenced from the X-ray structure, the Cu d_{z^2} orbital, which contains the unpaired electron, is directed along the Cu−O bond. Therefore, a spin polarization mechanism would cause the μ-hydroxo proton to be shielded and thus upfield shifted, as was previously reported for similar cases.[23] This observation is also consistent with the assignment.

The resonances E−G and C have been assigned to the pyridine protons according to their relative integral intensity of 2 (the intensity of C being measured at 233 K, where it appears relatively sharp). The resonances I and J, which overlap at 233 K, integrate as 4:4, as well as the resonances D and H and the two very broad resonances A and B. However, the integration of the latter two resonances is unfortunately rather ambiguous due to the line broadness, even when measured at 233 K.

Resonances D and H have been assigned to the protons of the pyrazole rings by ^{1}H 2D COSY NMR at 263 K (Figure

(25) Satcher, J. H. J.; Balch, A. L. *Inorg. Chem.* **1995**, *34*, 3371−3373.
(26) Aromi, G.; Gamez, P.; Kooijman, H.; Spek, A. L.; Driessen, W. L.; Reedijk, J. *Eur. J. Inorg. Chem.* **2003**, 1394−1400.

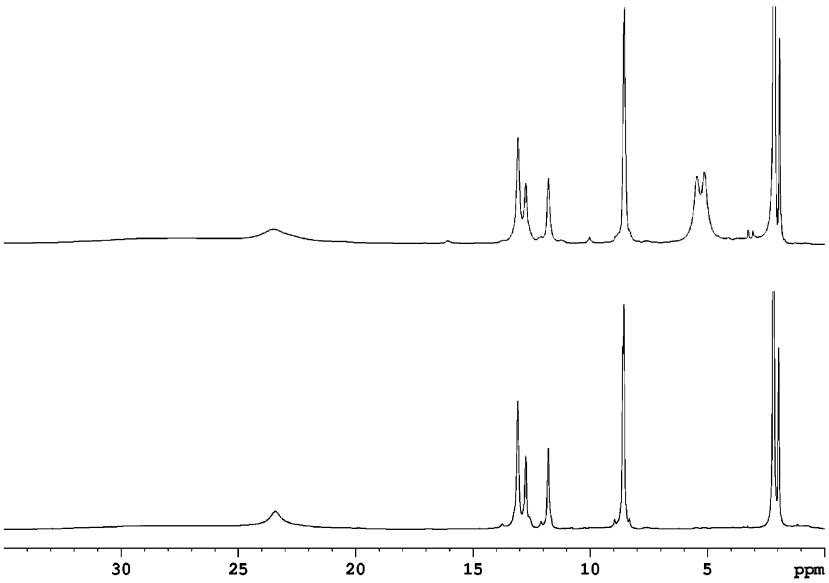

Figure 5. Positive range parts of the ^{1}H NMR spectra (300 MHz, CD_3CN) of **1** (top) and **1**-d_8 (bottom). (**1**-d_8 is the complex in which the protons of the ethylene moieties are substituted with deuterium atoms.)

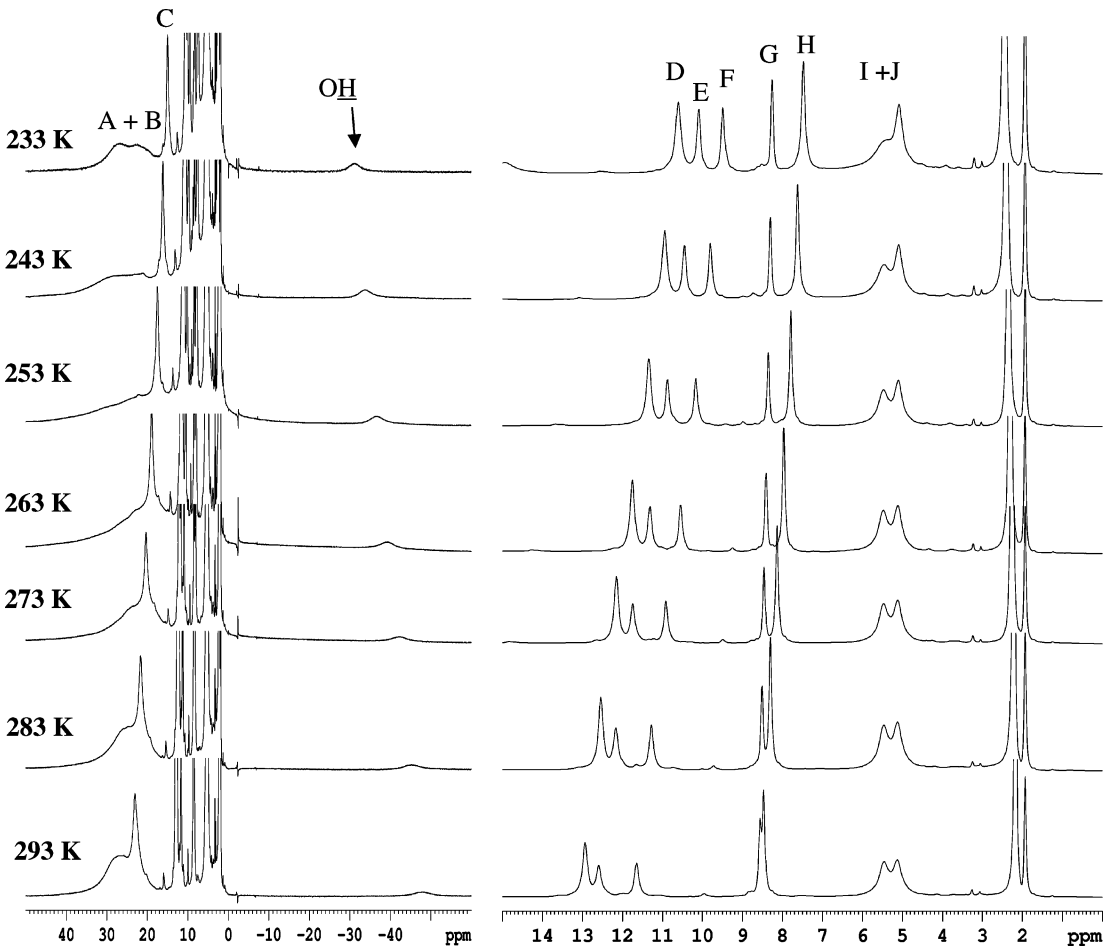

Figure 6. Changes in the ^{1}H NMR spectrum (300 MHz, CD_3CN) of **1** in the range 233−293 K: (left) whole spectrum range (+50 to −60 ppm), enlarged; (right) +15 to 0 ppm range.

7). The resonance G shows cross-signals with both resonances E and F, unambiguously ascribing it to the γ-protons of the pyridine rings and the resonances E and F to the *m*-pyridine protons. Resonances I and J, which do not display cross-signals in COSY, have been confirmed to originate from the diastereotopic ethylene protons by the substitution of the respective protons by deuterium. The signals in question are absent in the spectrum of the deuterated compound (Figure 5, bottom). Careful comparison of the Cu−H distances in the crystal structure indicates that the

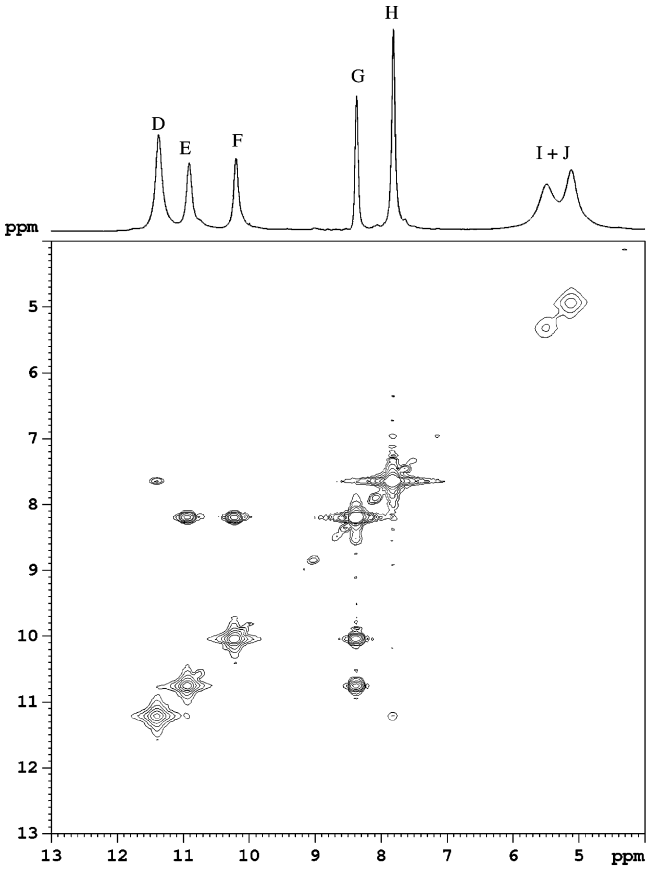

Figure 7. 2D COSY spectrum of **1** recorded at 263 K (CD_3CN, 300 MHz), displaying spin−spin connectivities between the resonances D and H and the resonances E and F and the resonance G.

protons H1b and H8b are located significantly closer to Cu(II) ions than their neighbors H1a and H8a. However, the corresponding resonances I and J are observed very close in the spectrum, which is perhaps caused by a rotational movement of the flexible ethylene groups of the complex cation in solution. The broad resonance A and B with the approximate integral intensity 4 can thus be assigned to the diastereotopic protons of the pyrazolylmethylene moieities, with axial protons experiencing larger hyperfine shifts than equatorial protons.[27] We believe that the resonance originating from the pyridylmethylene protons, which are closest to copper, is broadened beyond recognition; however, we should emphasize that a possibility of it being hidden under the resonances A and B cannot be ruled out, since the line broadness of the latter resonances makes their integration rather uncertain.

Further useful information can be obtained from the analysis of the longitudinal relaxation times (T_1). Assuming a predominant dipolar relaxation mechanism as reported by Holz and co-workers[21,23] in spin-coupled dicopper(II) complexes, the Cu−H distance r should be proportional to $T_1^{1/6}$. Using the equation $r_i = r_{ref}(T_{1i}/T_{1ref})^{1/6}$, in which r_i and T_{1i} are the Cu−H distance and the relaxation time of proton i and r_{ref} and T_{1ref} are the Cu−H distance and the relaxation time of the reference proton, the distances of each proton to the closest Cu(II) center can be calculated. As a reference proton the γ-proton of the pyridine ring was used, and r_{ref} was taken as an arithmetic average of the Cu−H distances of two equivalent γ-protons in the crystal structure. The results are listed in Table 3. As can be seen, in general a rather good correlation is observed between the solution-determined Cu−H distances and the crystallographic ones, as the discrepancies between the calculated and the observed Cu−H distances do not exceed 20%. The differences noted may originate from slight discrepancies between the solid-state and solution structures or from electron spin-delocalization and contact interactions within the aromatic rings. However, unfortunately the results do not allow the differentiation between the protons of the aromatic rings, e.g. 4′ and 5′ protons of the pyrazole rings and 3′ and 5′ protons of the pyridine rings.

Table 3. Longitudinal (T_1) Relaxation Times and Line Widths[a] Measured at 233 K and Cu−H Distances Calculated from the NMR Data for **1** and Determined from the X−ray Structure

reson	T_1 (ms)	line width (Hz)	r_{Cu-H}, calcd (Å)	r_{Cu-H}, determ (Å)	assgnt[d]
A	5.8	*b*	3.44	3.76	pz-C$H_{2(eq)}$-N
B	4.9	*b*	3.34	3.30	pz-C$H_{2(ax)}$-N
C	6.7	222	3.52	3.20	6′-H-py
D	68.0	46	5.18	4.96	4′-H-pz
E	58.8	27	5.06	4.90	3′-H-py
F	58.8	23	5.06	5.13	5′-H-py
G	132.6	13	5.79	5.79	4′-H-py
H	67.3	25	5.17	5.17	5′-H-pz
I	8.8	∼118[c]	3.69	3.36	Pz-$(CH_2)_2$-pz (H1b + H8b)
J	8.8	∼77[c]	3.69	4.61	Pz-$(CH_2)_2$-pz (H1a + H8a)

[a] The line widths are full width at half−maximum. [b] Not measured because of broadness. [c] Measured at 253 K due to the signals overlapping at 233 K. [d] See also Figure 8.

Resonance C, which does not show any cross-peaks in 2D COSY spectrum, probably due to its large line width, has been assigned to the 6′ pyridine protons by default. The lack of a cross-peak in 2D COSY NMR is not uncommon for α-pyridine protons of paramagnetic Cu(II) complexes.[21,23,28] The assignment is consistent with its T_1 and T_2 values (T_1 = 6.7 ms, T_2 = 222 Hz at 233 K) and its relatively large downfield shift in comparison to the other pyridine signals due to its close proximity to the copper(II) ions.

1D NOE Difference Measurements. In the case of paramagnetic metal complexes, the fast nuclear relaxation rates and the relatively small size of the molecules usually prevent the use of NOE techniques. This is caused by the fact that the NOE intensity in paramagnetic molecules is proportional to the rotational correlation time and inversely proportional to the nuclear relaxation rates.[29] Although 1D NMR techniques, like NOE difference spectroscopy, were previously successfully applied for the studies of biological proteins, they are scarcely used for the studies of coordination compounds.[30−34] To the best of our knowledge, we herein

(27) Belle, C.; Bougault, C.; Averbuch, M.-T.; Durif, A.; Pierre, J. L.; Latour, J. M.; Le Pape, L. *J. Am. Chem. Soc.* **2001**, *123*, 8053−8066.

(28) Lubben, M.; Hage, R.; Meetsma, A.; Bijma, K.; Feringa, B. L. *Inorg. Chem.* **1995**, *34*, 2217−2224.

(29) Bertini, I.; Luchinat, C. *NMR of Paramagnetic Molecules in Biological Systems*; Benjamin/Cummings: Menlo Park, CA, 1986.

(30) Epperson, J. D.; Ming, L.-J.; Woosley, B. D.; Baker, G. R.; Newkome, G. R. *Inorg. Chem.* **1999**, *38*, 4498−4502.

report the first example of NOE difference experiments being successfully applied on a paramagnetic Cu(II) complex, in an attempt to achieve a complete assignment of the resonances corresponding to the protons of the aromatic rings.

Irradiation of the resonances I and J at 263 K, corresponding to the protons of the ethylene moieties of the macrocyclic ring, yields in both cases positive NOE's for both resonances D and H (Figure S3, Supporting Information). The NOE signal of the latter resonance appears to be of higher intensity; therefore, we tentatively assign it to the 5′ protons of the pyrazole rings, which are located closer in space to the protons of the ethylene moieties. The very weak NOE signal of the resonance D is likely to be caused by spin diffusion. However, an absolute discrimination between these two resonances is unfortunately not possible, as the lower intensity of the NOE signal of the resonance D may also be inherent to its large line width.

It should be mentioned that the NOE connectivities between the pyrazole and ethylene protons are observed only upon irradiation of faster relaxing protons of the ethylene moieties (resonances I and J) but not upon irradiation of slower relaxing protons of the pyrazole rings (resonances D and H). In the case of the latter protons irradiation, only a positive NOE signal from the neighbor pyrazole proton is observed (Figure S4, Supporting Information). Similar behavior has been previously reported by Bubacco and coworkers for the Cu(II) active site of tyrosinase.[35]

Distinguishing between the 3′ and 5′ Protons of the Pyridine Rings. In the case of the 3′ and 5′ protons of the pyridine rings, the NOE spectroscopic technique could not be applied, as the only protons closely located to only one of the two considered protons are the protons of the pyridylmethylene moieties and the 6′ protons of the pyridine rings. While the protons of pyridylmethyl moieties are assumed to broaden beyond recognition, the very short T_1 value of the pyridine 6′ protons precluded an observation of appreciable NOE connectivities. Therefore, a derivative ligand in which the two 3′ protons of the pyridine rings were substituted by methyl groups was prepared. Regretfully, the very light-green compound obtained upon reaction of this ligand with copper(II) perchlorate in the presence of base in acetonitrile, exhibited very broad and poorly resolved resonances in the NMR spectrum in CD_3CN solution. In the UV−vis spectrum of this solution, the peak at 350 nm, corresponding to the CT band of the bridging OH^- to Cu(II) ions is absent, suggesting that the hydroxo-bridged complex with the methyl-substituted ligand does not form in acetonitrile. Fortunately, in D_2O, a reasonably well-resolved NMR spectrum could be recorded, which is shown in Figure S5 (bottom). The in situ formation of the hydroxo-bridged complex in D_2O was confirmed by UV−vis and mass spectroscopy (Experimental Section). For comparison, the spectrum of **1** was recorded in water as well (Figure S5, top). Although the quality of both spectra is rather poor, not in the least due to a poor solubility of the compounds, the two spectra are very similar. The absence of resonance E in the spectrum of the methylated complex allows its assignment to the 3′ protons of the pyridine rings in **1**. Another clear difference between the two spectra is the resolution of the resonances G and H in the spectrum of the complex with methylated ligand, in contrast to their degeneracy in the spectrum of **1** at RT (Figure S5). A very intensive peak of water traces, always present in D_2O, obscures the resonances I and J. A complete assignment of all resonances in ^1H NMR spectrum of **1** is shown in Figure 8.

Determination of the Antiferromagnetic Coupling Constant *J* from the Temperature-Dependent NMR Studies on 1. The temperature dependencies of the observed hyperfine-shifted NMR signals of **1** were recorded over the temperature range of 233−353 K. As can be seen from Figure 5, the resonances shift downfield with increasing temperature, the complex thus showing an anti-Curie behavior. As shown previously, the type of behavior in the antiferromagnetically coupled Cu(II) complexes was found to be dependent on the order of magnitude of the magnetic coupling constant J.[36] Antiferromagnetic coupling creates a dicopper(II) system in which the ground state ($S = 0$) is separated from the first excited ($S = 1$) state by $2J$.[37] A very elegant study reported by Shokhirev and Walker[38] takes into account the temperature-dependent change in the population of the excited state. This approach has been successfully used to evaluate the strength of the spin-coupling interaction for 2Fe−2S clusters and dicopper centers.[39,40] In the present case,

(31) Epperson, J. D.; Ming, L.-J.; Baker, G. R.; Newkome, G. R. *J. Am. Chem. Soc.* **2001**, *123*, 8583−8592.
(32) Dolores Santana, M.; Rufete, A.; Sanchez, G.; Garcia, G.; Lopez, G.; Casabo, J.; Molins, E.; Miravitlles, C. *Inorg. Chim. Acta* **1997**, *255*, 21−27.
(33) Momot, K. I.; Walker, F. A. *J. Phys. Chem. A* **1997**, *101*, 9207−9216.
(34) Lisowski, J.; Latos-Grazynski, L.; Szterenberg, L. *Inorg. Chem.* **1992**, *31*, 1933−1940.
(35) Bubacco, L.; Saldago, J.; Tepper, A. W. J. W.; Vijgenboom, E.; Canters, G. W. *FEBS Lett.* **1999**, *442*, 215−220.
(36) Holz, R. C.; Brink, J. M.; Rose, R. A. *J. Magn. Reson. A* **1996**, *119*, 125−128.
(37) Holz, R. C.; Alvarez, M. L.; Zumft, W. G.; Dooley, D. M. *Biochemistry* **1999**, *38*, 11164−11171.
(38) Shokhirev, N. V.; Walker, F. A. *J. Phys. Chem.* **1995**, *99*, 17795−17804.
(39) Holz, R. C.; Bennett, B.; Chen, G.; Ming, L.-J. *J. Am. Chem. Soc.* **1998**, *120*, 6329−6335.
(40) Holz, R. C.; Small, F. J.; Ensign, S. A. *Biochemistry* **1997**, *36*, 14690−14696.
(41) Haddad, M. S.; Wilson, S. R.; Hodgson, D. J.; Hendrickson, D. N. *J. Am. Chem. Soc.* **1981**, *103*, 384−391.
(42) Adams, H.; Bailey, N. A.; Collinson, S. R.; Fenton, D. E.; Haring, C. J.; Kitchen, S. J. *Inorg. Chim. Acta* **1996**, *246*, 81−88.
(43) Coughlin, P. K.; Lippard, S. J. *J. Am. Chem. Soc.* **1981**, *103*, 3228−3229.
(44) Lu, Q.; Latour, J.-M.; Harding, C. J.; Martin, N.; Marrs, D. J.; McKee, V.; Nelson, J. *J. Chem. Soc., Dalton Trans.* **1994**, 1471−1478.
(45) Harding, C. J.; McKee, V.; Nelson, J.; Lu, Q. *J. Chem. Soc., Chem. Commun.* **1993**, 1768−1769.
(46) Spodine, E.; Manzur, J.; Garland, M. T.; Kiwi, M.; Peña, O.; Grandjean, D.; Poupet, L. *J. Chem. Soc., Dalton Trans.* **1991**, 365−369.
(47) Drew, M. G. B.; McCann, M.; Martin-Nelson, M. *J. Chem. Soc., Dalton Trans.* **1981**, 1868−1878.
(48) Castro, I.; Faus, J.; Julve, M.; Lloret, F.; Verdaguer, M.; Kahn, O.; Jeannin, S.; Jeannin, Y.; Vaisserman, J. *J. Chem. Soc., Dalton Trans.* **1990**, 2207−2212.
(49) Foldago, J. V.; Coronado, E.; Beltran-Porter, D.; Rojo, T.; Fuertes, J. *J. Chem. Soc., Dalton Trans.* **1989**, 237−241.
(50) Harding, C. J.; Lu, Q.; Malone, J. F.; Marrs, D. J.; Martin, N.; McKee, V.; Nelson, J. *J. Chem. Soc., Dalton Trans.* **1995**, 1739−1747.

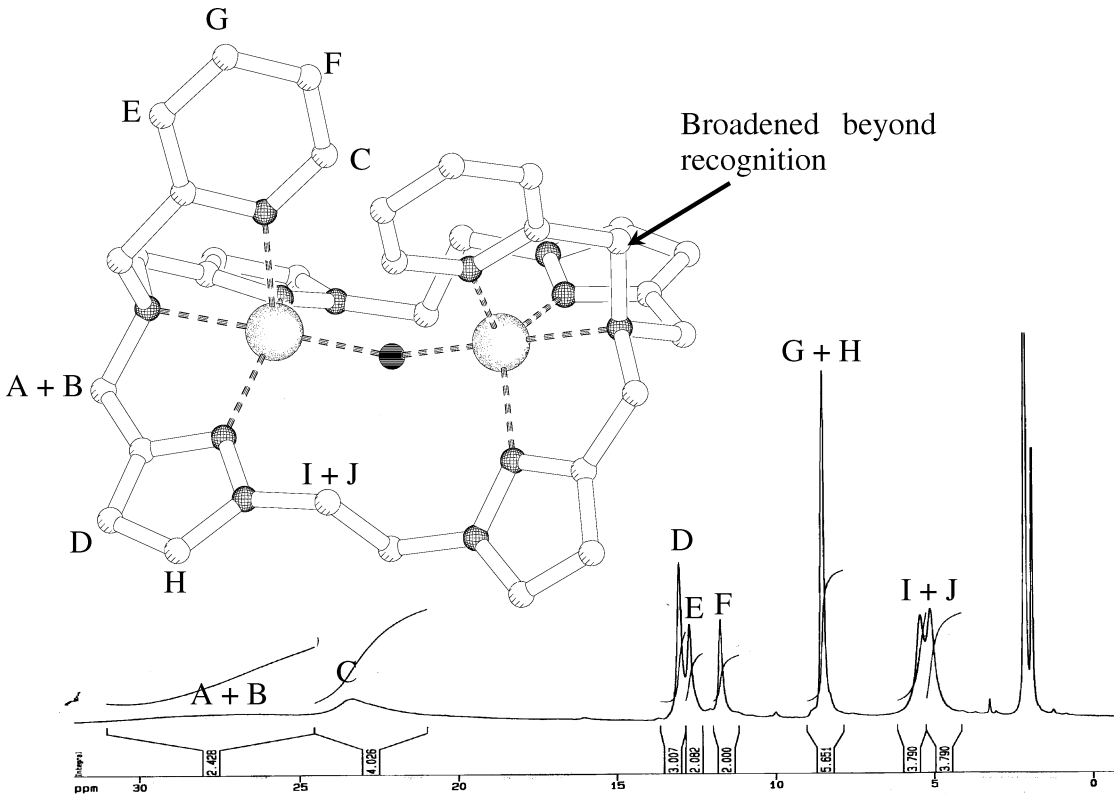

Figure 8. Assignment of the resonances in ^{1}H NMR spectrum of **1**. (See also Table 3.)

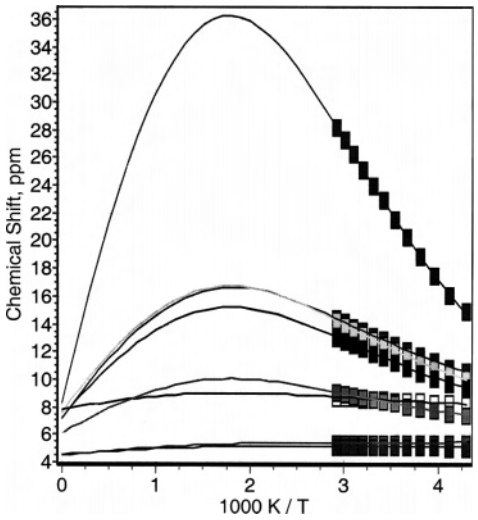

Figure 9. Plot of chemical shifts of **1** in the temperature range of 233−353 K vs the reciprocal temperature (1000 K/*T*). The simultaneous fitting for eight resonances by the program TDWf[38] results in $2J = -729(22)$ cm^{-1}.

the temperature data obtained for the hyperfine-shifted signals were simultaneously fit (Figure 9) using the program TDWf, kindly provided by Shokirev and Walker.[38] The fitting resulted in a $2J$ value of $-729(22)$ cm^{-1}. A relatively large error margin is due to the fitting of a limited temperature range, as dictated by the freezing and boiling temperatures of the solvent. Still, the obtained value is in perfect agreement with the exchange constant obtained from the magnetic susceptibility studies ($2J = -691(35)$ cm^{-1}). This result clearly demonstrates the possibility and power to use NMR spectroscopy to probe the magnetic properties of coordination compounds with unpaired electrons in solution.

Concluding Remarks

In conclusion, a monohydroxo bridge mediates an antiferromagnetic coupling between the metal centers in dinuclear Cu(II) complexes. Analysis of magneto−structural data for Cu(II) complexes with a single hydroxo bridge and different coordination geometries around Cu(II) ions (square-planar, square-pyramidal, and trigonal bipyramidal) indicates that, in all three cases, there is a common general trend with the strength of antiferromagnetic interaction increasing with longer Cu···Cu separations, wider Cu−O−Cu angles, and higher Cu−O−Cu/Cu···Cu ratios.

It can also be concluded that proton NMR spectroscopy is a valuable technique which can be successfully applied on paramagnetic Cu(II) complexes, provided that an antiferromagnetic coupling is present between the metal ions. The presence of strong antiferromagnetic interactions in a molecule overcomes the problem of long electron relaxation of the Cu(II) ions, leading to shorter longitudinal (T_1) and transversal (T_2) nuclear relaxation times. As a result, commonly used NMR techniques for diamagnetic molecules, like 2D COSY and 1D NOE difference measurements, can also be successfully applied on Cu(II) complexes. In particular, the latter spectroscopic technique can potentially be a rich source of structural information in solution. Finally, the strength of the magnetic coupling between the metal ions can be determined rather precisely from solution NMR studies. There is little doubt that NMR spectroscopy will

(51) Asato, E.; Toftlund, H.; Kida, S.; Mikuriya, M.; Murray, K. S. *Inorg. Chim. Acta* **1989**, *165*, 207−214.

further develop as one of the most successful tools to study the structural and magnetic properties of paramagnetic molecules in solution.

Acknowledgment. Support of the NRSC Catalysis (a Research School Combination of HRSMC and NIOK) is kindly acknowledged. Also support and sponsorship concerted by COST Action D21/003/2001 is gratefully acknowledged. A collaborative travel grant from the French Ministry of Research and Foreign Affairs and NWO (Van Gogh Program), allowing visits and exchanges between Leiden and Grenoble, is gratefully acknowledged. We are very much indebted to F. Lefeber and K. Erkelens for their help in the NMR studies.

Supporting Information Available: Crystallographic details for complex **1** in CIF format, a figure depicting a correlation of the singlet−triplet energy gap 2*J* in monohydroxo-bridged dicopper(II) complexes with the Cu−O−Cu angle for different Cu coordination geometries, and a figure depicting field dependence of the magnetization of **1** at 5 and 100 K, showing the presence of a small paramagnetic impurity. Figures depicting the NOE difference spectra obtained upon irradiation of the resonances I and J, and the resonances H and D, and a figure depicting 1H NMR spectrum of the complex with the methylated ligand. This material is available free of charge via the Internet at http://pubs.acs.org.

IC0501770